Research Square

Preprints are preliminary reports that have not undergone peer review.
They should not be considered conclusive, used to inform clinical practice,
or referenced by the media as validated information.

Ni-catalyzed Electrochemical Cross-Electrophile Coupling Paired with Oxygen Evolution Reaction

Renyi Shi

renyi.shi@xjtu.edu.cn

Xi'an Jiaotong University https://orcid.org/0000-0002-7359-0043

Donghao Huo

Xi'an Jiaotong University

Wenjing Li

Xi'an Jiaotong University

Rui Ma

Xi'an Jiaotong University

Shentong Xie

Xi'an Jiaotong University

Pengcheng Wang

Nanjing University of Science and Technology https://orcid.org/0000-0002-5282-236X

Aiwen Lei

Wuhan University https://orcid.org/0000-0001-8417-3061

Article

Keywords:

Posted Date: October 21st, 2025

DOI: https://doi.org/10.21203/rs.3.rs-7763126/v1

License: This work is licensed under a Creative Commons Attribution 4.0 International License.
Read Full License

Additional Declarations: There is **NO** Competing Interest.

Abstract

Nickel-catalyzed cross-electrophile coupling (XEC) has emerged as an efficient and economical strategy for constructing C–C bonds, a pivotal transformation in diversifying molecular architectures. However, conventional XEC methodologies typically rely on stoichiometric metallic reductants, which present inherent challenges including safety risks, operational instability, and environmental concerns. Although electrochemical XEC in undivided cells circumvents the need for chemical reductants, it remains constrained by sustainability issues and chemo-selectivity limitations due to its dependence on sacrificial metal anodes or stoichiometric organic donors to supply electrons for cathodic reduction. Herein, we report a nickel-catalyzed electrochemical cross-electrophile coupling paired with the oxygen evolution reaction (OER). By utilizing water as an economical and sustainable sacrificial electron donor, this electrochemical platform facilitates the versatile construction of diverse C–C bonds, including Csp^2–Csp^3, Csp^3–Csp^3, and Csp–Csp^3 linkages, from readily accessible aryl, alkenyl, alkynyl, and alkyl halide electrophiles, affording products in yields up to 99%. The undivided cell configuration markedly reduces system complexity, lowers capital costs, and supports scalable electrochemical synthesis. Moreover, this electroreductive coupling strategy exhibits broad functional group tolerance and is amenable to the late-stage derivatization of complex drugs and natural products. This operationally simple, electricity-driven approach offers a sustainable and versatile platform for C–C bond formation.

Introduction

Carbon–carbon (C–C) bonds constitute essential structural motifs in pharmaceuticals, agrochemicals, and functional materials, serving as central scaffolds in numerous bioactive molecules.[1,2] Conventional methodologies for constructing these bonds predominantly employ transition-metal-catalyzed cross-coupling reactions between organohalide electrophiles and preformed organometallic nucleophiles.[3–9] However, the reliance on such carbon nucleophiles—which themselves often necessitate pre-synthesis from organohalides—introduces synthetic inefficiencies and operational complexities. In response, cross-electrophile coupling (XEC) has emerged as an efficient alternative strategy, enabling the direct coupling of two electrophilic coupling partners.[7,10–21] The most prevalent XEC paradigm employs nickel catalysis paired with stoichiometric metallic reductants such as manganese or zinc powders (Fig. 1a). Nevertheless, this approach suffers from several limitations that impede scalable implementation: inconsistent reactivity due to variations in metal particle morphology and surface passivation, practical difficulties in homogenizing high-density metal powders in batch reactors, and the generation of stoichiometric quantities of metal waste. These drawbacks have stimulated growing interest in electrochemical strategies as more sustainable and scalable avenues for XEC transformations.

Electrochemical synthesis offers a promising platform for developing sustainable routes to industrial chemicals, presenting distinct advantages over traditional methods that often involve hazardous reagents or energy-intensive processes.[21–26] Anodic oxidation reactions, in particular, exhibit a favorable environmental profile, as they can frequently be conducted under reagent-free conditions with

molecular hydrogen (H_2) generated as the sole byproduct at the counter electrode.[27,28] In contrast, reductive electrochemical cross-electrophile couplings conducted in undivided cells pose significant sustainability challenges due to their inherent demand for an external electron source to drive the cathodic transformation. At the laboratory scale, this electron requirement is typically supplied by sacrificial metal anodes or stoichiometric organic reductants.[29–44] While operationally simple for small-scale applications, such strategies become economically and environmentally prohibitive at scale due to the substantial consumption of sacrificial materials and concomitant generation of metal-containing waste or organic byproducts (Fig. 1b). To address these issues, Stahl and co-workers reported a mediated H_2 anode that achieves indirect electrochemical oxidation of H_2 by pairing thermal catalytic hydrogenation of an anthraquinone mediator with electrochemical oxidation of the anthrahydroquinone.[39] This quinone-mediated H_2 anode is used to support nickel-catalysed electrochemical cross-electrophile couplings.

In contrast to the electrochemical hydrogen oxidation reaction (HOR), which requires gaseous H_2 and specialized electrode architectures, the oxygen evolution reaction (OER)—involving the oxidation of water to molecular oxygen—represents a more sustainable and practically viable anodic process.[45,46] However, the implementation of OER in electrochemical cross-electrophile couplings faces two critical challenges: (i) the compatibility between aqueous OER and organic electrochemical reactions, and (ii) suppression of competitive substrate, product, or catalyst oxidation due to a more anodic the high operating potential required for OER (Fig. 1c). The potential for OER in organic solvents can be described by the following expression:

$$\mathrm{E\,(OER)} = \mathrm{E^{\circ}\ (OER)} + \frac{RT}{nF} ln \frac{\left[\mathrm{H^{+}}\right]}{\left[\mathrm{H_2O}\right]} + \eta$$

where E^{o}(OER), R, T, n, F and η represent the thermodynamic standard potential of OER (about + 0.59 V vs. Fc/Fc^{+}), gas constant, temperature, number of the electron transfer, Faraday constant and over potential respectively. This equation indicates that the OER potential in organic media is highly dependent on concentration of proton, concentration of water, and the electrocatalytic properties of the anode material, which determines the value of η. We hypothesized that these challenges could be mitigated through careful regulation of water content, screening of alkaline additives, and optimization of anode materials. Herein, we report a Ni-catalyzed electrochemical cross-electrophile coupling that facilitates C–C bond formation paired with oxygen evolution reaction (Fig. 1d). This strategy circumvents the need for sacrificial metal anodes or stoichiometric organic reductants, offering a more sustainable and operationally simplified approach to reductive cross-coupling.

Results and discussion

To establish a general protocol for Ni-catalyzed electrochemical cross-electrophile coupling employing water as a sacrificial reductant, methyl 4-iodobenzoate (aryl halide, **1a**) and 4-iodotetrahydropyran (alkyl

halide, **2a**) were selected as model substrates. The initial reaction conditions employed $NiCl_2$·dme (10 mol%) as the precatalyst, dtbpy (15 mol%) as the ligand, LiOTf (0.2 M) as the electrolyte, and DMA (6 mL) as the solvent, with a Pt anode, carbon felt cathode, and a constant current of 30 mA (Scheme 1a). Water was identified as a critical sacrificial reductant for achieving high efficiency. Consequently, the effect of water equivalents was systematically evaluated. In the absence of added water, the reaction proceeded at room temperature for 4 hours to afford methyl 4-(tetrahydro-2H-pyran-4-yl)benzoate (3a) in 37% GC yield, presumably due to trace moisture present in the solvent. The low yield (3%) obtained when using anhydrous DMA as the solvent underscores the critical role of water as a sacrificial anode reagent in this reaction. The product yield increased significantly with higher water loading, reaching an optimum of 86% with 30 equivalents. A further increase to 1 mL of water resulted in a notable decrease in yield, likely attributable to compromised solubility of organic reactants. Subsequent efforts focused on reducing concentration of proton by the introduction of base to lower the potential of oxygen evolution reaction (OER) (Scheme 1b). The addition of 20% sodium carbonate enhanced the yield of **3a** to 99% (Entry 1). Alternative basic additives, including Cs_2CO_3 and NaOH, were evaluated but proved detrimental to reactivity (Entries 2 and 3). Replacement of the Pt anode with an IrO_2 electrode—an efficient OER catalyst—yielded only trace product, likely owing to incompatibility with the organic medium (Entry 4). Other anode materials such as gold and carbon felt also exhibited inferior performance (Entries 5 and 6). Control experiments underscored the essential roles of the nickel catalyst, ligand, and electrochemical activation. No product formation was observed in the absence of $NiCl_2$·dme, dtbpy, or applied current (Entries 7–9).

With the optimized reaction conditions in hand, we systematically evaluated the generality and functional group compatibility of the nickel-catalyzed electrochemical cross-electrophile coupling using water as a sacrificial reductant. Initially, the coupling between various aryl iodides and alkyl iodides was investigated (Scheme 2a). Aryl iodides bearing electron-withdrawing groups like ester (**3a**–**3c**), trifluoromethyl (**3d**, **3e**), and cyano (**3f**) were well tolerated. Substitutions at the *meta*-position of the phenyl ring significantly influenced the reaction yields (**3c**), whereas *ortho*-substituents led to a slight decrease in yield (**3b**, **3e**), indicating notable steric effects. Notably, aryl iodides containing halogen substituents such as -F, -Cl, and even -Br proved to be suitable substrates, offering handles for further functionalization (**3g**–**3i**). Electron-rich aryl iodides also underwent smooth coupling, affording products in moderate yields (**3j**–**3p**). To our delight, substrates with unprotected amino groups were compatible, delivering 4-(tetrahydro-2H-pyran-4-yl)aniline in 81% yield (**3q**). Substrate containing oxidation-sensitive functional groups like aldehyde could be successfully employed in the divided cell system, thereby delivering the desired products in moderate yields (**3r**). The Bpin group was also tolerated under the standard conditions (**3s**). Furthermore, complex aromatic systems including biphenyl (**3t**), naphthalene (**3u**), and dimethylfluorene (**3v**) served as viable coupling partners. Indole, a privileged scaffold in bioactive molecules, was also compatible with this electrochemical system (**3w**).

As summarized in Scheme 2b, the reaction exhibited broad compatibility with diverse alkyl iodides. Secondary cyclic alkyl iodides including four-membered (**3x**), five-membered (**3y**), six-membered (**3z**),

and seven-membered rings (**3aa**) underwent efficient coupling, demonstrating insensitivity to ring size and strain. 5-Iodo-2-phenyl-1,3-dioxane was also a suitable substrate, affording the product in moderate yield (**3ab**). Primary alkyl iodides performed well, affording methyl 4-(3-(p-tolyl)propyl)benzoate in 97% yield (**3ac**). The method further displayed excellent functional group tolerance on the alkyl partner, successfully accommodating chloride (**3ad**), nitrile (**3ae**), thioether (**3af**), ether (**3ag**), -CF_3 (**3ah**), thiophene (**3ai**), and furan (**3aj**) functionalities.

To further demonstrate the versatility of this electrochemical cross-coupling system, we expanded its scope to include alkyl-alkyl electrophilic couplings, encompassing both primary–secondary and primary–primary alkyl partners (Scheme 3a, 3**ak** and **3al**). The protocol was also successfully applied to alkenyl bromides, affording the desired product in 61% yield (**3am**). Additionally, the system proved effective for the construction of Csp–Csp^3 bonds, yielding disubstituted alkynes (**3an**). Notably, the method was compatible with less reactive aryl bromides under the standard electrochemical conditions. A range of substituted aryl bromides including those bearing esters, fluorine, and chlorine underwent efficient coupling with both primary and secondary alkyl iodides to deliver the corresponding products in moderate yields (**3a**, **3g**, **3h**, **3u**, **3ao**, **3y**). The synthetic utility of this methodology was further highlighted through the late-stage functionalization of complex bioactive molecules and natural product derivatives (Scheme 3b). Successful couplings were achieved with substrates derived from Gemfibrozil (**3ap**), Clofibrate (**3aq**, **3ar**) and Ibuprofen (**3as**). These transformations proceeded efficiently, underscoring the potential of this electrochemical strategy for the modular functionalization of pharmacologically relevant compounds.

To assess the scalability of the electrochemical cross-coupling, a gram-scale reaction was performed at 10 mmol scale under slightly modified conditions (constant current: 100 mA). The desired coupled product was isolated in 58% yield (1.36 g), demonstrating the practical utility of this method for larger-scale synthesis (Scheme 4, Eq. 1). This approach offers a direct route to alkyl–aryl linkages from carboxylic acid derivatives, eliminating the need for preformed alkyl halides (Scheme 4, Eq. 2). To probe the reaction mechanism, a series of control experiments were conducted. Analysis of the headspace gas via GC during the standard reaction confirmed the evolution of oxygen (0.18 mmol), supporting the occurrence of the oxygen evolution reaction (OER) under the electrochemical conditions (Scheme 4, Eq. 3). The addition of stoichiometric TEMPO completely inhibited product formation, suggesting the involvement of radical intermediates (Scheme 4, Eq. 4). This hypothesis was further corroborated by the reaction of methyl 4-iodobenzoate (**1a**) with (iodomethyl)cyclopropane, which yielded the ring-opened product **3at**, consistent with the generation of a primary alkyl radical that undergoes rapid ring fragmentation (Scheme 4, Eq. 5).

Further mechanistic insight was gained through cyclic voltammetry (CV) studies (Fig. 2). In the presence of ligand, the Ni complex exhibited two reduction peaks at -1.19 V and − 1.88 V (vs. Ag/AgCl), attributed to the Ni^{II}/Ni^{I} and Ni^{I}/Ni^{0} redox couples, respectively (Fig. 2a). The reduction potentials of iodobenzene and 4-iodotetrahydropyran were observed at -2.22 V and − 2.16 V (vs. Ag/AgCl), respectively, indicating that reduction of the $NiCl_2$·dme/dtbpy complex occurs more readily than that of the organic iodides.

Upon addition of iodobenzene, a catalytic current increase was observed for the Ni^{I}/Ni^{0} couple, while the Ni^{II}/Ni^{I} couple remained largely unaffected, suggesting that oxidative addition of aryl iodide preferentially occurs at Ni^{0} (Fig. 2b). In contrast, introduction of 4-iodotetrahydropyran led to an increase in catalytic current for both the Ni^{II}/Ni^{I} and Ni^{I}/Ni^{0} redox events, indicating that alkyl iodides are more likely to react with Ni^{I} species (Fig. 2c).

Based on the results described above, a plausible mechanism is proposed as shown in Fig. 3. Cathodic reduction of catalyst precursor generates an active Ni^{0} species (**A**), which undergoes oxidative addition with aryl iodide (Ar-I) to form an aryl-Ni^{II}-I intermediate (**B**). Subsequent electrochemical reduction yields an aryl-Ni^{I}-I complex (**C**), which participates in single-electron transfer (SET) with alkyl iodide (R-I) to generate an alkyl radical (R•) and regenerate aryl-Ni^{II}-I (**D**). Radical capture affords a high-valent Ar-Ni^{III}-R species (**E**), and reductive elimination delivers the coupled product while regenerating a Ni^{I} intermediate (**F**). The Ni^{I} species is reduced at the cathode to Ni^{o}, regenerating the catalyst.

Conclusions

In summary, we have developed a novel nickel-catalyzed electroreductive cross-coupling method for C–C bond formation, using H_2O as an economical and sustainable sacrificial reductant. This electrochemical platform enables the versatile construction of diverse C–C bonds including Csp^2–Csp^3, Csp^3–Csp^3, and Csp–Csp^3 linkages, from readily accessible aryl, alkenyl, alkynyl, and alkyl halide electrophiles, delivering products in yields of up to 99%. The approach eliminates the need for sacrificial metal anodes or stoichiometric organic reductants, offering a more sustainable and operationally straightforward alternative for cross-electrophile coupling. Furthermore, this electroreductive coupling strategy displays excellent functional group tolerance and is suitable for the late-stage derivatization of complex drugs and natural products. This operationally simple, electricity-driven method provides a sustainable and versatile platform for C–C bond formation. We anticipate that this strategy will find broad utility in synthetic and medicinal chemistry.

Declarations

Competing interests

The authors declare no competing interests.

Author contributions

R.S. directed the project. A.L. and R.S. conceived the idea, designed the experiments and wrote the manuscript. D.H., W.L. and R.M. performed the synthetic experiments. All the authors participated in the

discussion and preparation of the manuscript.

Acknowledgements

This work is supported by the “Young Talent Support Plan” of Xi’an Jiaotong University and the Natural Science Foundation of Shaanxi Province (2023-JC-QN-0102).

Data availability

The authors declare that the data supporting the findings of this study are available within the article and Supplementary Information files or from the corresponding author upon request. The experimental procedures and characterization of all new compounds are provided in the Supplementary Information.

References

1. Lovering, F.; Bikker, J.; Humblet, C. Escape from Flatland: Increasing Saturation as an Approach to Improving Clinical Success, *J. Med. Chem.* **2009**, *52*, 6752–6756.
2. Lovering, F. Escape from Flatland 2: complexity and promiscuity, *Med. Chem. Commun.* **2013**, *4*, 515–519.
3. Miyaura, N.; Suzuki, A. Palladium-Catalyzed Cross-Coupling Reactions of Organoboron Compounds, *Chem. Rev.* **1995**, *95*, 2457–2483.
4. Netherton, M. R.; Fu, G. C. Nickel-Catalyzed Cross-Couplings of Unactivated Alkyl Halides and Pseudohalides with Organometallic Compounds, *Adv. Synth. Catal.* **2004**, *346*, 1525–1532.
5. Phapale, V. B.; Cárdenas, D. J. Nickel-catalysed Negishi cross-coupling reactions: scope and mechanisms, *Chem. Soc. Rev.* **2009**, *38*, 1598–1607.
6. Jana, R.; Pathak, T. P.; Sigman, M. S. Advances in Transition Metal (Pd,Ni,Fe)-Catalyzed Cross-Coupling Reactions Using Alkyl-organometallics as Reaction Partners, *Chem. Rev.* **2011**, *111*, 1417–1492.
7. Cherney, A. H.; Kadunce, N. T.; Reisman, S. E. Enantioselective and Enantiospecific Transition-Metal-Catalyzed Cross-Coupling Reactions of Organometallic Reagents To Construct C–C Bonds, *Chem. Rev.* **2015**, *115*, 9587–9652.
8. Choi, J.; Fu, G. C. Transition metal–catalyzed alkyl-alkyl bond formation: Another dimension in cross-coupling chemistry, *Science* **2017**, *356*, eaaf7230.
9. Chen, Z.; Rong, M.-Y.; Nie, J.; Zhu, X.-F.; Shi, B.-F.; Ma, J.-A. Catalytic alkylation of unactivated C(sp3)–H bonds for C(sp3)–C(sp3) bond formation, *Chem. Soc. Rev.* **2019**, *48*, 4921–4942.
10. Everson, D. A.; Weix, D. J. Cross-Electrophile Coupling: Principles of Reactivity and Selectivity, *J. Org. Chem.* **2014**, *79*, 4793–4798.

11. Knappke, C. E. I.; Grupe, S.; Gärtner, D.; Corpet, M.; Gosmini, C.; Jacobi von Wangelin, A. Reductive Cross-Coupling Reactions between Two Electrophiles, *Chem. Eur. J.* **2014**, *20*, 6828–6842.
12. Gu, J.; Wang, X.; Xue, W.; Gong, H. Nickel-catalyzed reductive coupling of alkyl halides with other electrophiles: concept and mechanistic considerations, *Org. Chem. Front.* **2015**, *2*, 1411–1421.
13. Hanna, L. E.; Jarvo, E. R. Selective Cross-Electrophile Coupling by Dual Catalysis, *Angew. Chem., Int. Ed.* **2015**, *54*, 15618–15620.
14. Weix, D. J. Methods and Mechanisms for Cross-Electrophile Coupling of Csp2 Halides with Alkyl Electrophiles, *Acc. Chem. Res.* **2015**, *48*, 1767–1775.
15. Lucas, E. L.; Jarvo, E. R. Stereospecific and stereoconvergent cross-couplings between alkyl electrophiles, *Nat. Rev. Chem.* **2017**, *1*, 0065.
16. Liu, J.; Ye, Y.; Sessler, J. L.; Gong, H. Cross-Electrophile Couplings of Activated and Sterically Hindered Halides and Alcohol Derivatives, *Acc. Chem. Res.* **2020**, *53*, 1833–1845.
17. Zhou, Z.; Xu, S.; Zhang, J.; Kong, W. Nickel-catalyzed enantioselective electroreductive cross-couplings, *Org. Chem. Front.* **2020**, *7*, 3262–3265.
18. Xue, W.; Jia, X.; Wang, X.; Tao, X.; Yin, Z.; Gong, H. Nickel-catalyzed formation of quaternary carbon centers using tertiary alkyl electrophiles, *Chem. Soc. Rev.* **2021**, *50*, 4162–4184.
19. Chen, H.; Yue, H.; Zhu, C.; Rueping, M. Reactivity in Nickel-Catalyzed Multi-component Sequential Reductive Cross-Coupling Reactions, *Angew. Chem. Int. Ed.* **2022**, *61*, e202204144.
20. Pang, X.; Su, P.-F.; Shu, X.-Z. Reductive Cross-Coupling of Unreactive Electrophiles, *Acc. Chem. Res.* **2022**, *55*, 2491–2509.
21. Yi, L.; Ji, T.; Chen, K.-Q.; Chen, X.-Y.; Rueping, M. Nickel-catalyzed reductive cross-couplings: new opportunities for carbon-carbon bond formations through photochemistry and electrochemistry, *CCS Chem.* **2022**, *4*, 9–30.
22. Moeller, K. D. Synthetic Applications of Anodic Electrochemistry, *Tetrahedron* **2000**, *56*, 9527–9554.
23. Yoshida, J.-i.; Kataoka, K.; Horcajada, R.; Nagaki, A. Modern Strategies in Electroorganic Synthesis, *Chem. Rev.* **2008**, *108*, 2265–2299.
24. Francke, R.; Little, R. D. Redox catalysis in organic electrosynthesis: basic principles and recent developments, *Chem. Soc. Rev.* **2014**, *43*, 2492–2521.
25. Yan, M.; Kawamata, Y.; Baran, P. S. Synthetic Organic Electrochemical Methods Since 2000: On the Verge of a Renaissance, *Chem. Rev.* **2017**, *117*, 13230–13319.
26. Novaes, L. F. T.; Liu, J.; Shen, Y.; Lu, L.; Meinhardt, J. M.; Lin, S. Electrocatalysis as an enabling technology for organic synthesis, *Chem. Soc. Rev.* **2021**, *50*, 7941–8002.
27. Yuan, Y.; Lei, A. Electrochemical Oxidative Cross-Coupling with Hydrogen Evolution Reactions, *Acc. Chem. Res.* **2019**, *52*, 3309–3324.
28. Yuan, Y.; Yang, J.; Lei, A. Recent advances in electrochemical oxidative cross-coupling with hydrogen evolution involving radicals, *Chem. Soc. Rev.* **2021**, *50*, 10058–10086.

29. Chaussard, J.; Folest, J.-C.; Nedelec, J.-Y.; Perichon, J.; Sibille, S.; Troupel, M. Use of Sacrificial Anodes in Electrochemical Functionalization of Organic Halides, *Synthesis* **1990**, *1990*, 369–381.
30. Franke, M. C.; Weix, D. J. Recent Advances in Electrochemical, Ni-Catalyzed C − C Bond Formation, *Isr. J. Chem.* **2024**, *64*, e202300089.
31. Nedelec, J. Y.; Mouloud, H. A. H.; Folest, J. C.; Perichon, J. Electrochemical cross-coupling of alkyl halides in the presence of a sacrificial anode, *J. Org. Chem.* **1988**, *53*, 4720–4724.
32. Perkins, R. J.; Pedro, D. J.; Hansen, E. C. Electrochemical Nickel Catalysis for Sp2-Sp3 Cross-Electrophile Coupling Reactions of Unactivated Alkyl Halides, *Org. Lett.* **2017**, *19*, 3755–3758.
33. Perkins, R. J.; Hughes, A. J.; Weix, D. J.; Hansen, E. C. Metal-Reductant-Free Electrochemical Nickel-Catalyzed Couplings of Aryl and Alkyl Bromides in Acetonitrile, *Org. Process Res. Dev.* **2019**, *23*, 1746–1751.
34. Kurimoto, A.; Sherbo, R. S.; Cao, Y.; Loo, N. W. X.; Berlinguette, C. P. Electrolytic deuteration of unsaturated bonds without using D2, *Nature Catal.* **2020**, *3*, 719–726.
35. Hamby, T. B.; LaLama, M. J.; Sevov, C. S. Controlling Ni redox states by dynamic ligand exchange for electroreductive Csp3–Csp2 coupling, *Science* **2022**, *376*, 410–416.
36. Harwood, S. J.; Palkowitz, M. D.; Gannett, C. N.; Perez, P.; Yao, Z.; Sun, L.; Abruña, H. D.; Anderson, S. L.; Baran, P. S. Modular terpene synthesis enabled by mild electrochemical couplings, *Science* **2022**, *375*, 745–752.
37. Zhang, W.; Lu, L.; Zhang, W.; Wang, Y.; Ware, S. D.; Mondragon, J.; Rein, J.; Strotman, N.; Lehnherr, D.; See, K. A.; Lin, S. Electrochemically driven cross-electrophile coupling of alkyl halides, *Nature* **2022**, *604*, 292–297.
38. Li, P.; Kou, G.; Feng, T.; Wang, M.; Qiu, Y. Electrochemical NiH-Catalyzed C(sp3) − C(sp3) Coupling of Alkyl Halides and Alkyl Alkenes, *Angew. Chem. Int. Ed.* **2023**, *62*, e202311941.
39. Twilton, J.; Johnson, M. R.; Sidana, V.; Franke, M. C.; Bottecchia, C.; Lehnherr, D.; Lévesque, F.; Knapp, S. M. M.; Wang, L.; Gerken, J. B.; Hong, C. M.; Vickery, T. P.; Weisel, M. D.; Strotman, N. A.; Weix, D. J.; Root, T. W.; Stahl, S. S. Quinone-mediated hydrogen anode for non-aqueous reductive electrosynthesis, *Nature* **2023**, *623*, 71–76.
40. Bu, F.; Deng, Y.; Xu, J.; Yang, D.; Li, Y.; Li, W.; Lei, A. Electrocatalytic reductive deuteration of arenes and heteroarenes, *Nature* **2024**, *634*, 592–599.
41. Cardinale, L.; Beutner, G. L.; Bemis, C. Y.; Weix, D. J.; Stahl, S. S. Non-Innocent Role of Sacrificial Anodes in Electrochemical Nickel-Catalyzed C(sp2)–C(sp3) Cross-Electrophile Coupling, *J. Am. Chem. Soc.* **2024**, *146*, 32249–32254.
42. Li, P.; Zhu, Z.; Guo, C.; Kou, G.; Wang, S.; Xie, P.; Ma, D.; Feng, T.; Wang, Y.; Qiu, Y. Nickel-electrocatalysed C(sp3)–C(sp3) cross-coupling of unactivated alkyl halides, *Nature Catal.* **2024**, *7*, 412–421.
43. Xie, S.; Yin, Y.; Wang, Y.; Wang, J.; He, X.; Bai, R.; Shi, R. Current-controlled nickel-catalyzed multi-electrophile electroreductive cross-coupling, *Green Chem.* **2023**, *25*, 1522–1529.

44. Xie, S.; Lu, M.; Wang, P.; Shi, R. Current-Regulated Selective Nickel-Catalyzed Electroreductive Cross-Electrophile Carbonylation to β/γ-Hydroxy Ketones, *Angew. Chem. Int. Ed.* **2025**, *64*, e202418147.
45. Song, J.; Wei, C.; Huang, Z. F.; Liu, C.; Zeng, L.; Wang, X.; Xu, Z. J. A review on fundamentals for designing oxygen evolution electrocatalysts, *Chem. Soc. Rev.* **2020**, *49*, 2196–2214.
46. Yuan, Y.; Li, J.; Zhu, Y.; Qiao, Y.; Kang, Z.; Wang, Z.; Tian, X.; Huang, H.; Lai, W. Water in Electrocatalysis, *Angew. Chem. Int. Ed.* **2025**, *64*, e202425590.
47. Magee, P. N.; Barnes, J. M. Carcinogenic nitroso compounds, *Adv. Cancer Res.* **1967**, *10*, 163–246.
48. Shank, R. C. Toxicology of N-nitroso compounds, *Toxicol. Appl. Pharmacol.* **1975**, *31*, 361–368.
49. DeRubertis, F. R.; Craven, P. A. Calcium-independent modulation of cyclic GMP and activation of guanylate cyclase by nitrosamines, *Science* **1976**, *193*, 897–899.
50. Hecht, S. S. Biochemistry, biology, and carcinogenicity of tobacco-specific N-nitrosamines, *Chem. Res. Toxicol.* **1998**, *11*, 559–603.
51. Manchuri, K. M.; Shaik, M. A.; Gopireddy, V. S. R.; Sultana, N.; Gogineni, S. Analytical Methodologies to Detect N-Nitrosamine Impurities in Active Pharmaceutical Ingredients, Drug Products and Other Matrices, *Chem. Res. Toxicol.* **2024**, *37*, 1456–1483.
52. Schlingemann, J.; Burns, M. J.; Ponting, D. J.; Martins Avila, C.; Romero, N. E.; Jaywant, M. A.; Smith, G. F.; Ashworth, I. W.; Simon, S.; Saal, C.; Wilk, A. The Landscape of Potential Small and Drug Substance Related Nitrosamines in Pharmaceuticals, *J. Pharm. Sci.* **2023**, *112*, 1287–1304.
53. Liu, J. K.-Y.; Feng, E.; Fu, Y.; Li, W.; Ma, X.; Sheng, H.; Kong, J.; Liu, Y.; Hicks, M.; Xiang, B.; Liu, Z.; Pennington, J.; Kenttämaa, H. I. A Diagnostic Nitrosamine Detection Approach for Pharmaceuticals by Using Tandem Mass Spectrometry Based on Diagnostic Gas-Phase Ion-Molecule Reactions, *Anal. Chem.* **2022**, *94*, 13795–13803.
54. Marlés-Torres, A.; López-García, R.; Bessa-Jambrina, S.; Galán-Rodríguez, C. Ultra-high-speed liquid chromatography combined with mass spectrometry detection analytical methods for the determination of nitrosamine drug substance-related impurities, *J. Sep. Sci.* **2023**, *46*, e2300125.
55. Shuker, D. E. G.; Tannenbaum, S. R. Determination of nonvolatile N-nitroso compounds in biological fluids by liquid chromatography with postcolumn photohydrolysis detection, *Anal. Chem.* **1983**, *55*, 2152–2155.
56. Fine, D. H.; Lieb, D.; Rufeh, F. Principle of operation of the thermal energy analyzer for the trace analysis of volatile and non-volatile N-nitroso compounds, *J. Chromatogr. A* **1975**, *107*, 351–357.
57. Xu, G.; Reed, P. I. Method for group determination of total N-nitroso compounds and nitrite in fresh gastric juice by chemical denitrosation and thermal energy analysis, *Analyst* **1993**, *118*, 877–883.
58. Wang, J.; Chan, W. G.; Haut, S. A.; Krauss, M. R.; Izac, R. R.; Hempfling, W. P. Determination of Total N-Nitroso Compounds by Chemical Denitrosation Using CuCl, *J. Agric. Food Chem.* **2005**, *53*, 4686–4691.
59. Wang, Q.-H.; Yu, L.-J.; Liu, Y.; Lin, L.; Lu, R.-g.; Zhu, J.-p.; He, L.; Lu, Z.-L. Methods for the detection and determination of nitrite and nitrate: A review, *Talanta* **2017**, *165*, 709–720.

60. Wang, Z.; Xu, P.; Guo, S.-M.; Daniliuc, C. G.; Studer, A. C-to-N atom swapping and skeletal editing in indoles and benzofurans, *Nature* **2025**, *642*, 92–98.
61. Chow, Y. L. Carbon-Carbon Double Bond Cleavage by Photoaddition of N-Nitrosodialkylamine to Olefins, *J. Am. Chem. Soc.* **1965**, *87*, 4642–4643.
62. Chow, Y. L.; Wu, Z. Z. Light-induced self-nitrosation of polycyclic phenols with nitrosamine. Excited state proton transfer, *J. Am. Chem. Soc.* **1987**, *109*, 5260–5267.
63. Bohle, D. S.; Chua, Z.; Perepichka, I.; Rosadiuk, K. Lewis acid stabilization and activation of primary N-nitrosamides, *RSC Adv.* **2017**, *7*, 8205–8219.
64. Galloway, J. D.; Sarabia, C.; Fettinger, J. C.; Hratchian, H. P.; Baxter, R. D. Versatile New Reagent for Nitrosation under Mild Conditions, *Org. Lett.* **2021**, *23*, 3253–3258.
65. Patil, D. V.; Si, T.; Kim, H. Y.; Oh, K. Visible-Light-Induced Photoaddition of N-Nitrosoalkylamines to Alkenes: One-Pot Tandem Approach to 1,2-Diamination of Alkenes from Secondary Amines, *Org. Lett.* **2021**, *23*, 3105–3109.
66. Yuan, P.-F.; Huang, T.; He, J.; Huang, X.-T.; Jin, X.-L.; Sun, C.; Wu, L.-Z.; Liu, Q. Controllable Z/E-selective synthesis of α-amino-ketoximes from N-nitrososulfonamides and aryl alkenes under neutral conditions, *Org. Chem. Front.* **2021**, *8*, 5785–5792.
67. Patil, D. V.; Lee, Y.; Kim, H. Y.; Oh, K. Visible-Light-Promoted Photoaddition of N-Nitrosopiperidines to Alkynes: Continuous Flow Chemistry Approach to Tetrahydroimidazo[1,2-a]pyridine 1-Oxides, *Org. Lett.* **2022**, *24*, 5840–5844.
68. Sureshbabu, P.; Bhajammanavar, V.; Choutipalli, V. S. K.; Subramanian, V.; Baidya, M. Unorthodox cascade reaction of arynes and N-nitrosamides leading to indazole scaffolds, *Chem. Commun.* **2022**, *58*, 1187–1190.
69. Huang, T.; Yuan, P.-F.; Dong, K.; Zong, Y.-Y.; Liu, C.; Wang, R.-H.; Jin, X.-L.; Liu, Q. A Barton nitrite ester-type remote functionalization and cyclization of N-nitrosobenzamides, *Org. Chem. Front.* **2023**, *10*, 4559–4564.
70. Wang, Z.; Wierich, N.; Zhang, J.; Daniliuc, C. G.; Studer, A. Alkyl Radical Generation from Alkylboronic Pinacol Esters through Substitution with Aminyl Radicals, *J. Am. Chem. Soc.* **2023**, *145*, 8770–8775.
71. Chen, Y.; Peng, R.-j.; Zhang, X.-j.; Yan, M. Transition-metal catalyzed reactions of diazo compounds and N,N-dialkylnitrosoamines, *Org. Chem. Front.* **2024**, *11*, 176–182.
72. Lan, H.; Huo, X.; Jia, Y.; Wang, D. Silyl Radical Generation from Silylboronic Pinacol Esters through Substitution with Aminyl Radicals, *Org. Lett.* **2024**, *26*, 1011–1016.
73. Lan, H.; Su, Y.; Chen, Y.; He, X.; Wang, D. A general photochemical strategy for the oximation of activated alkenes without a catalyst, *Org. Chem. Front.* **2024**, *11*, 4207–4213.
74. Yuan, P.-F.; Huang, X.-T.; Long, L.; Huang, T.; Sun, C.-L.; Yu, W.; Wu, L.-Z.; Chen, H.; Liu, Q. Regioselective Dearomative Amidoximation of Nonactivated Arenes Enabled by Photohomolytic Cleavage of N-nitrosamides, *Angew. Chem. Int. Ed.* **2024**, *63*, e202317968.

75. Sang, J.-W.; Zhang, Y.; Xia, D.; Hu, Z.; Wang, J.; Zhang, W.-D. Photomediated controllable alkylation/nitrosoalkylation of N-heteroaromatics via nucleohomolytic substitution of alkylboronic esters with N-nitrosamines, *Org. Chem. Front.* **2025**, *12*, 869–878.
76. Wang, P. G.; Xian, M.; Tang, X.; Wu, X.; Wen, Z.; Cai, T.; Janczuk, A. J. Nitric Oxide Donors: Chemical Activities and Biological Applications, *Chem. Rev.* **2002**, *102*, 1091–1134.
77. Adam, W.; Krebs, O. The Nitroso Ene Reaction: A Regioselective and Stereoselective Allylic Nitrogen Functionalization of Mechanistic Delight and Synthetic Potential, *Chem. Rev.* **2003**, *103*, 4131–4146.
78. Yamamoto, H.; Momiyama, N. Rich chemistry of nitroso compounds, *Chem. Commun.* **2005**, 3514–3525.
79. Hartung, J. Organic Radical Reactions Associated with Nitrogen Monoxide, *Chem. Rev.* **2009**, *109*, 4500–4517.
80. Beard, J. C.; Swager, T. M. An Organic Chemist's Guide to N-Nitrosamines: Their Structure, Reactivity, and Role as Contaminants, *J. Org. Chem.* **2021**, *86*, 2037–2057.
81. Ieda, N.; Yoshikawa, Y.; Tomita, N.; Ohkubo, K.; Hotta, Y.; Kawaguchi, M.; Kimura, K.; Nakagawa, H. Ascorbate-assisted nitric oxide release from photocontrollable nitrosonium ion releasers for potent ex vivo photovasodilation, *Chem. Commun.* **2022**, *58*, 8420–8423.
82. Soto, J. Identification of the Photoreactive Species of Protonated N-Nitrosopiperidine in Acid Medium: A CASPT2 and DFT Study, *J. Phys. Chem. A* **2023**, *127*, 9781–9786.
83. Chen, Z.-L.; Li, Q.-Q.; Studer, A.; Xuan, J. Emerging progress: photochemical transformation of nitroso compounds, *Sci. China Chem.* **2025**, *68*, 118–133.
84. Xu, T.; Cheung, C. W.; Hu, X. Iron-Catalyzed 1,2-Addition of Perfluoroalkyl Iodides to Alkynes and Alkenes, *Angew. Chem. Int. Ed.* **2014**, *53*, 4910–4914.
85. Guo, Q.; Wang, M.; Liu, H.; Wang, R.; Xu, Z. Visible-Light-Promoted Dearomative Fluoroalkylation of β-Naphthols through Intermolecular Charge Transfer, *Angew. Chem. Int. Ed.* **2018**, *57*, 4747–4751.
86. Postigo, A. Electron Donor-Acceptor Complexes in Perfluoroalkylation Reactions, *Eur. J. Org. Chem.* **2018**, *2018*, 6391–6404.
87. Helmecke, L.; Spittler, M.; Baumgarten, K.; Czekelius, C. Metal-Free Activation of C–I Bonds and Perfluoroalkylation of Alkenes with Visible Light Using Phosphine Catalysts, *Org. Lett.* **2019**, *21*, 7823–7827.
88. Lu, K.; Wei, X.; Li, Q.; Li, Y.; Ji, L.; Hua, E.; Dai, Y.; Zhao, X. Synthesis of α-trifluoromethyl ethanone oximes via the three-component reaction of aryl-substituted ethylenes, tert-butyl nitrite, and the Langlois reagent, *Org. Chem. Front.* **2019**, *6*, 3766–3770.
89. Wu, Y.; Zhang, Y.; Yang, Z.; Jiao, J.; Zheng, X.; Feng, W.; Zhang, M.; Cheng, H.; Tang, L. Dual Roles of tert-Butyl Nitrite in the Transition Metal- and External Oxidant-Free Trifluoromethyloximation of Alkenes, *ChemSusChem* **2019**, *12*, 3960–3966.
90. Zheng, D.; Studer, A. Photoinitiated Three-Component α-Perfluoroalkyl-β-heteroarylation of Unactivated Alkenes via Electron Catalysis, *Org. Lett.* **2019**, *21*, 325–329.

91. Chen, Y.-L.; Han, W.; Ren, Y.-Y.; Ma, M.; Ge, D.; Shen, Z.-L.; Guo, K.; Chu, X.-Q. Defluorinative Cyclization of Enamides with Fluoroalkyl Halides Through Two Vicinal C(sp^3)–F Bonds Functionalization, *Adv. Sci.* **2025**, *12*, 2404738.
92. Guo, K.; Liu, S.; Yang, Y.; Xu, F.; Lu, Y.; Shang, J.; Song, A. Photoredox/Copper Dual-Catalyzed Three-Component Perfluoroalkyl Trifluoromethylthiolation of Alkenes, *Org. Lett.* **2025**, *27*, 1994–1998.
93. Jiang, J.; Dai, H.; Tu, T. Two vicinal C(sp^3)-F bonds functionalization of perfluoroalkyl halides (PFAHs), *Chin. Chem. Lett.* **2025**, *36*, 111054.
94. Li, C.; Chen, N.; Yao, T.; Zhao, C.; Liao, S.; Song, Q. Remote Boryl and Alkenyl Radical Migration of Olefin-Bearing Aryl Bromides, *CCS Chem.* **2025**, *7*, 279–292.
95. Yang, K.; Zhang, F.; Fang, T.; Zhang, G.; Song, Q. Stereospecific 1,4-Metallate Shift Enables Stereoconvergent Synthesis of Ketoximes, *Angew. Chem. Int. Ed.* **2019**, *58*, 13421–13426.
96. Zard, S. Z. Recent progress in the generation and use of nitrogen-centred radicals, *Chem. Soc. Rev.* **2008**, *37*, 1603–1618.

Schemes

Schemes 1 and 4 are available in the Supplementary Files section

Figures

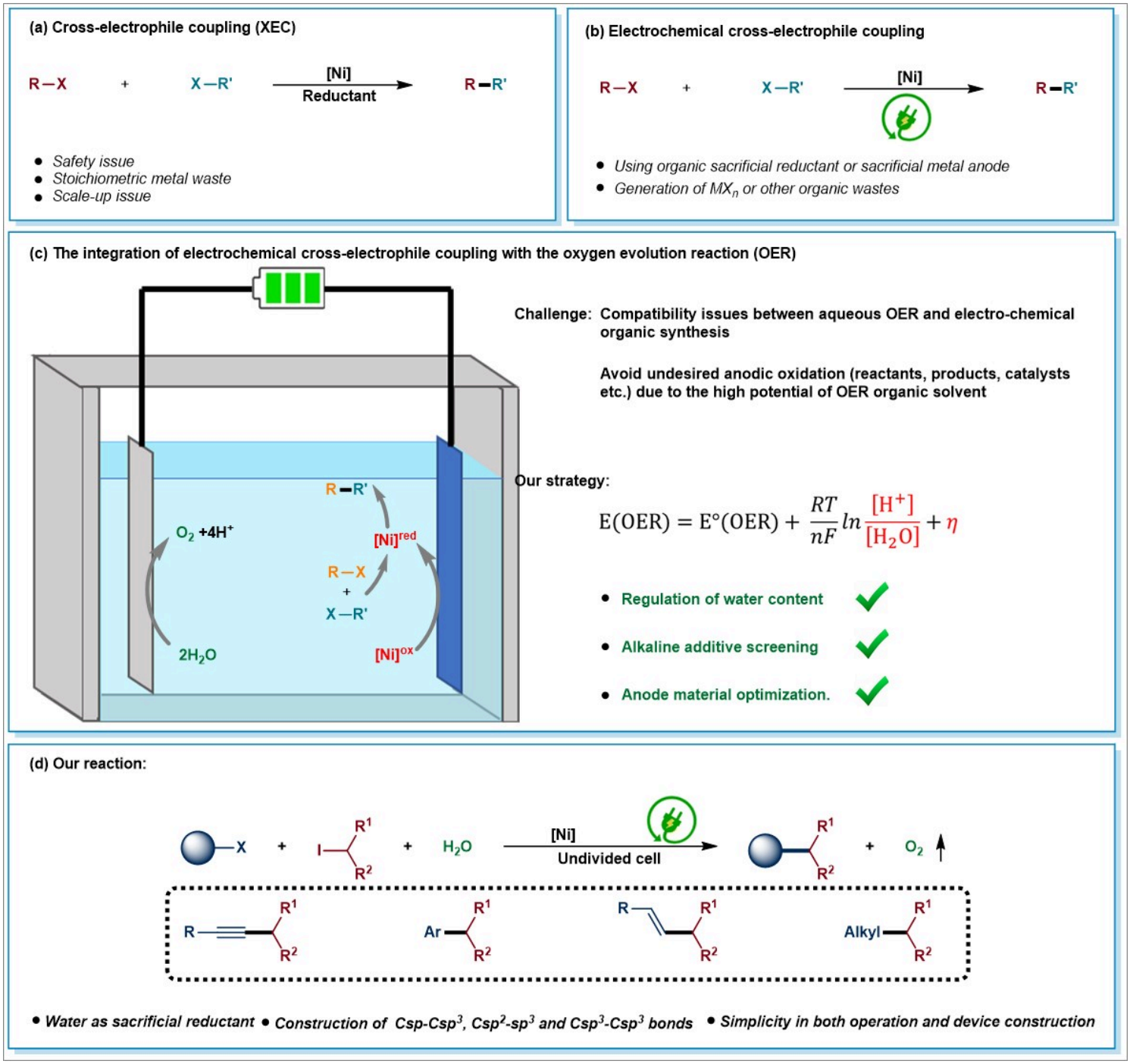


Figure 1

(a) Cross-electrophile coupling (XEC). (b) Electrochemical cross-electrophile coupling. (c) The integration of electrochemical cross-electrophile coupling with the oxygen evolution reaction (OER). (d) Our reaction.

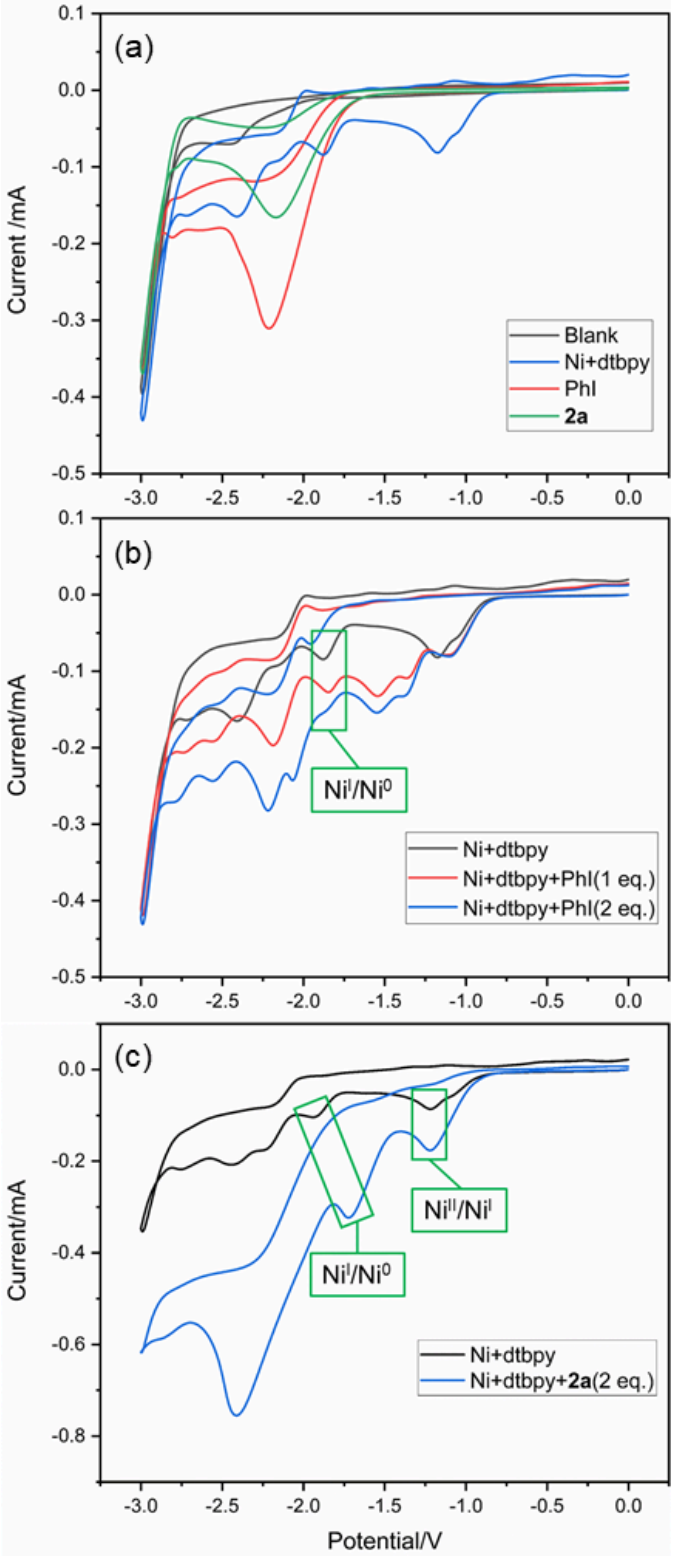


Figure 2

Cyclic voltammetry experiments.

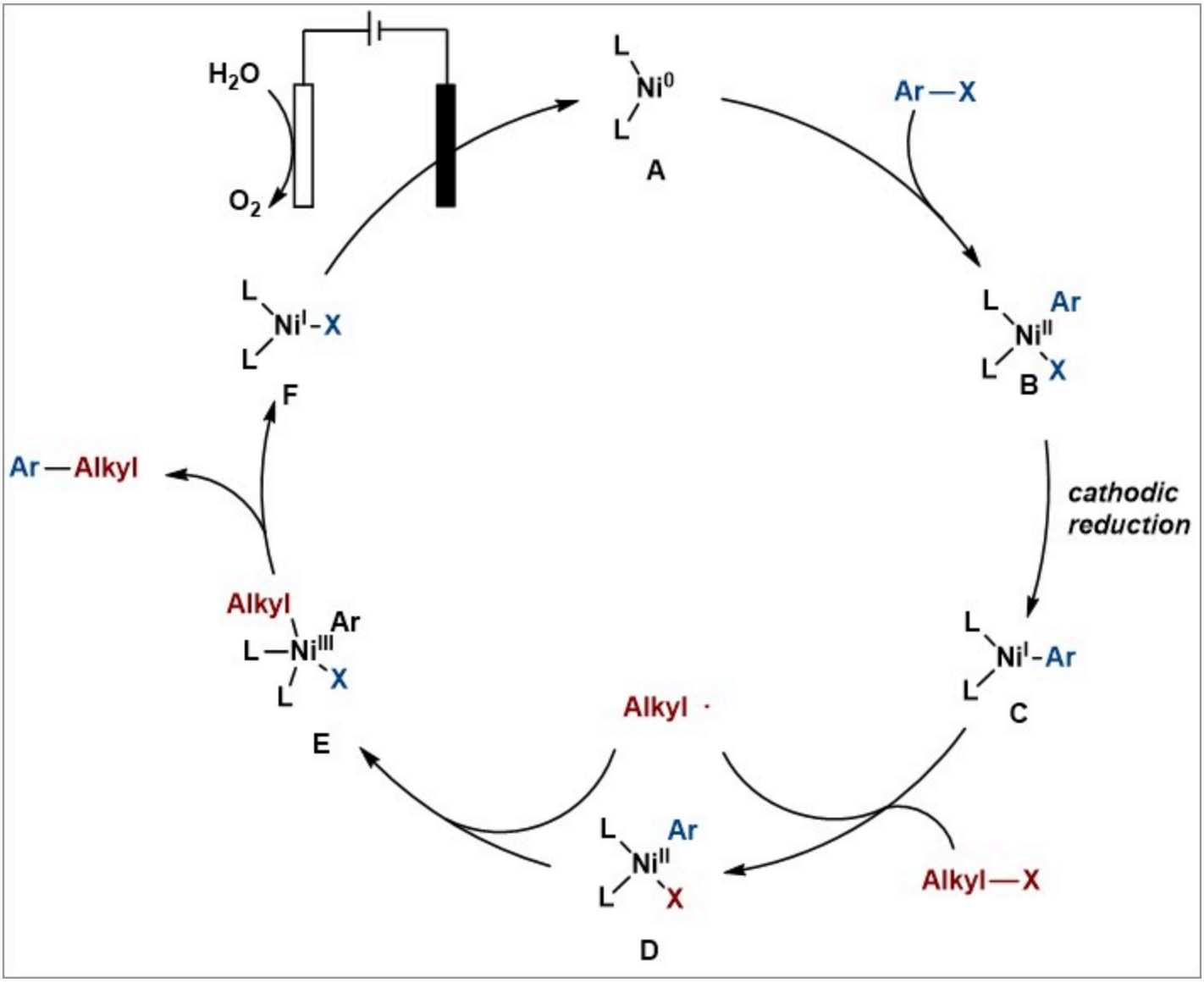


Figure 3

Proposed mechanism

Supplementary Files

This is a list of supplementary files associated with this preprint. Click to download.

- supportinginformation.pdf
- GA.png
- SC1.png
- SC2.png
- SC3.png
- SC4.png